

Probing the Nature of EROs through ASTRO-F/AKARI observations

A.Mignano¹, P.Saracco¹, M.Longhetti¹
 1. INAF, OAB, Milano, Italy

1. Abstract

We present a preliminary analysis of ASTRO-F data of a complete sample of ~ 150 EROs ($R-K > 5$) down to $K < 19$, expected in the redshift range $0.8 < z < 2$, selected over two fields (S7 and S2) of MUNICS survey. The area covered is of about 420 arcmin^2 . We have imaged this area with AKARI telescope in N3 ($3.4 \mu\text{m}$), N60 ($65 \mu\text{m}$) and WL ($150 \mu\text{m}$) down to $5 \mu\text{Jy}$ in the N3 filter, in order to detect the rest frame H or K-band emission, thus providing an excellent sampling of the SED of our EROs. From the first analysis we have an identification rate of $\sim 63\%$ in the N3 filter over the S7 field.

These data should allow us to distinguish starburst from passive early type phenomena, to measure the SFR of the starburst component and to constrain the dust content of starburst EROs.

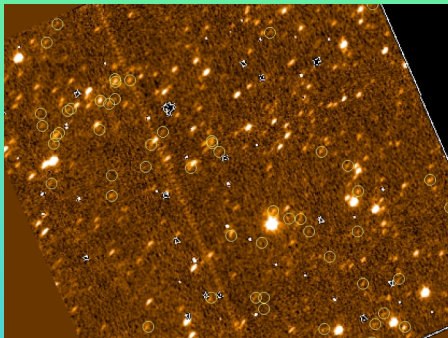
2. Introduction

While the general build-up of cosmic structures seems to be well described by hierarchical model of galaxy formation (ΛCDM), the assembly of the baryonic mass on galactic scale still represents a weak point of the galaxy formation models. One of these difficulties consists in explaining the large population of Extremely Red Objects ($R-K > 5$) EROs. This population is a mixture of early type galaxies and dusty star-forming. The hierarchical models should reproduce the abundance of massive red galaxies at $1 < z < 2$ and balance among the number of early type and obscured star-forming galaxies (Nagamine et al. 2005).

Since the mid-IR observations are usually not available for large samples of EROs, the rest frame H-K emission is extrapolated from the observed optical emission (partially affected by extinction) which is dominated by young stars ($< 0.5\text{-}1\text{Gyr}$). As the EROs are mainly composed of old stars, the reliability of stellar masses is extremely uncertain.

The way to provide the models with robust observational constraints passes through mid-IR observations of a large (> 100), bright ($K < 19$) and complete sample of EROs.

Fig.1 The S7F5 field imaged with N3 filter (IRC camera). The yellow circle represent the EROs selected from MUNICS catalog \rightarrow



3. The Sample

We selected a complete sample of ~ 150 EROs ($R-K > 19$) at $K < 19$ over two well separated fields (S7 and S2) of MUNICS survey (Drory et al. 2001). This area ($\sim 420 \text{ arcmin}^2$) and the redshift range ($0.8 < z < 2$) covered by our sample imply a volume larger than 10^6 Mpc^3 . The MUNICS provides multiband information (B,V,R,I,J,K) down to limiting magnitudes 25,24,23,21,19.5 (Vega, Drory et al. 2001).

We have imaged this area with the AKARI telescope in N3 ($3.4 \mu\text{m}$), N60 ($65 \mu\text{m}$) and WL ($150 \mu\text{m}$) down to $5 \mu\text{Jy}$ in the N3 filter.

In this work we present the preliminary analysis made on the N3 images of S7 field (Fig. 1), where 65 EROs are present.

To identify the N3 counterparts of our selected EROs the nearest mid-IR object was searched for. Figure 2 shows the mid-IR optical distance distribution of the N3 counterparts. As can be seen most of identification are found within $3.5''$. Beyond this distance the distribution is flat as expected for spurious identifications. Thus, we identify 41/65 EROs with a success rate of 63% . This value is lower than what expected on the basis of AKARI Exposure Time Calculator. It means that the N3 images are shallower by a factor ~ 2 .

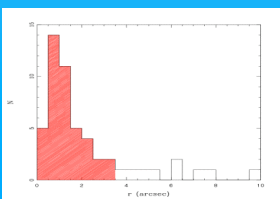


Fig.2 N3 counterparts distribution vs r . We consider as "good identifications" the ones within $3.5''$ from the optical object (red histogram). \leftarrow

4. Sample Composition

We run the Hyperz (Bolzonella et al. 2000) routine to assess the spectral type of our 41 identified EROs. We used a template with an exponentially declining SFR with e -folding time ($\tau = 0.1\text{Gyr}$) and $A_V < 0.2$ to describe the early type galaxies and a constant star formation with $A_V < 2.0$ to describe star forming galaxies. The templates are provided by the Bruzual & Charlot (2007) library. The spectral type is assigned by the fit with the lowest reduced χ^2 value. 35 objects (85% of the whole sample) were classified as ETG (Early Type Galaxies), while the 6 (15%) as SFG (Star Forming Galaxies). In Fig.3 we show respectively an example for ETG and SFG galaxy. We stress that part of the SFG component can be misclassified by the routine, thus explaining their low number.

In Fig. 4 we show the J-K vs. R-K colours of our sample. The solid line represent the border between passively evolving and star forming galaxies (Mannucci et al 2002). Also plotted the evolutionary tracks for ETG (blue line) and SFG (red line) in the redshift range $0.8 < z < 2$. Our classification is in agreement with the Mannucci plots with a considerable number of galaxies very close to the partition line.

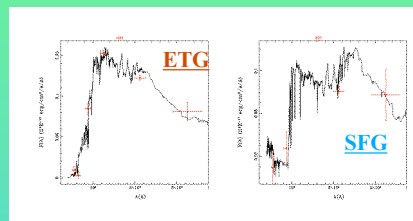


Fig.3 Examples of fitting with SEDs of SFG and ETG.

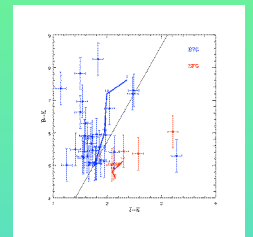


Fig.4 J-K vs R-K colours for the 41 identified EROs. Solid line divides the two different classes of ETG (blue points) and SFG (red points)

5. Stellar Mass Density

We calculated the Stellar Mass for each galaxy from the best fitting model.

In Fig.4 we show the distribution of stellar masses for the two different population, while in Fig.5 we show the evolution in z of the stellar mass density compared with other literature values.

We obtained a stellar mass density $\rho_{\text{star}} = (2.3 \pm 0.4) \cdot 10^7 M_{\text{sun}} \text{ Mpc}^3$ in good agreement with other estimates.

On the basis of our results, there is no evolution till $z \sim 1.3$ in the stellar mass density of the ETG population, constraining the assembly of such objects to $z > 1.5-2$.

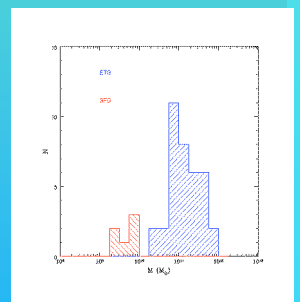


Fig.4 Distribution of Stellar Mass for ETG (blue dashed histogram) and for SFG (red dashed histogram).

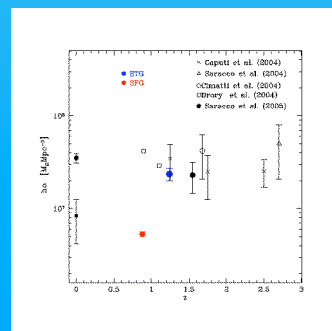


Fig.5 Stellar Mass Density vs. z for ETG (blue point) and for SFG (red point), compared with other literature values. \leftarrow